A Feasibility Study on Network NOMA

Yanshi Sun, Zhiguo Ding, *Senior Member, IEEE*, Xuchu Dai, and George K. Karagiannidis, *Fellow, IEEE*

***Abstract*— To study the feasibility of network non-orthogonal multiple access (N-NOMA) techniques, this paper proposes a N-NOMA scheme for a downlink coordinated multipoint (CoMP) communication scenario, with randomly deployed users. In the considered N-NOMA scheme, superposition coding (SC) is employed to serve cell-edge users as well as users close to base stations (BSs) simultaneously, and distributed analog beamforming by the BSs to meet the cell-edge user's quality of service requirements. The combination of SC and distributed analog beamforming significantly complicates the expressions for the signal-to-interference-plus-noise ratio at the receiver, which makes the performance analysis particularly challenging. However, by using rational approximations, insightful analytical results are obtained in order to characterize the outage performance of the considered N-NOMA scheme. Computer simulation results are provided to show the superior performance of the proposed scheme as well as to demonstrate the accuracy of the analytical results.**

***Index Terms*— Network non-orthogonal multiple access (N-NOMA), coordinated multipoint (CoMP), network multiple-input multiple-output (network MIMO), superposition coding (SC).**

I. Introduction

NON-ORTHOGONAL multiple access (NOMA) has been recognized as a promising multiple access technique for the fifth generation (5G) mobile networks, due to its superior spectral efficiency [1]–[3]. By using NOMA, multiple users can be served simultaneously at the same time, frequency, and spreading code. The key idea of NOMA is to apply superposition coding (SC) at the transmitter in order to efficiently mix multiple users' signals [4], [5]. Furthermore, at the transmitter, NOMA power allocation is utilized by exploiting the difference among the users' channel conditions, i.e., users with poorer channel conditions are allocated more transmission power. On the other hand, at the receiver side, users with better channel conditions apply successive interference cancellation (SIC) in order to separate the received mixture [6].

The performance of NOMA with randomly deployed users has been studied in [7], and the user fairness of NOMA was investigated in [8]. In [9], the impact of user pairing on NOMA has been studied, where the power allocation coefficients are chosen to meet the predefined users' quality of service (QoS) requirements. Furthermore, the design of uplink NOMA has been proposed and studied in [10], while the application of multiple-input multiple-output (MIMO) technologies to NOMA has been studied in [11]–[13]. Recently, NOMA has been applied to massive MIMO and millimeter wave (mmWave) networks [14], as well as to visible light communications [15].

Network MIMO is a family of smart antenna techniques, where each user in a wireless system is served by multiple base stations (BSs) or access points (APs), which are within the service range of the user [16], [17]. As a typical representative of network MIMO, coordinated multipoint (CoMP) has been recognized as an important enhancement for LTE-A [18]–[20]. The main benefit to use CoMP is to improve the cell-edge users' data rates and hence improve the cell coverage. For CoMP transmission in downlink, various schemes can be applied, such as dynamic cell selection and coordinated beamforming [21], [22]. A drawback of these schemes is, that all the associated BSs need to allocate the same channel resource block with the cell-edge user. When orthogonal multiple access (OMA) is used, this channel resource block cannot be accessed by other users, and hence, the spectral efficiency becomes worse as the number of cell-edge users increases. In order to deal with this problem, network NOMA (N-NOMA) has been proposed for CoMP [23], [24]. In [23], NOMA with SC was employed in a CoMP system with two BSs to provide robust service to cell-edge users and to users close to BSs concurrently. Furthermore, in [23], Alamouti code, originally proposed in [25], has been applied to improve the cell-edge user's reception reliability. In [24], NOMA with opportunistic BS or AP selection has been studied for CoMP. Both schemes in [23] and [24] enlarges the system throughput, which demonstrates the superior performance of N-NOMA.

This paper proposes a novel N-NOMA scheme for a downlink CoMP system with randomly deployed users. The users are divided into two categories: the cell-edge users and the near users. The cell-edge users are far from the BSs and are with strict QoS requirements, while the near users are close to the BSs and are served opportunistically. The contributions of this paper are listed as follow.

- A downlink CoMP transmission system with three BSs and randomly deployed users, is considered. A novel

Manuscript received November 19, 2017; revised February 28, 2018; accepted April 4, 2018. Date of publication April 11, 2018; date of current version September 14, 2018. The work of Y. Sun and X. Dai was supported by the National Natural Science Foundation of China under Grant 61471334. The work of Z. Ding was supported by the UK EPSRC under grant number EP/L025272/1 and by H2020-MSCA-RISE-2015 under grant number 690750. The associate editor coordinating the review of this paper and approving it for publication was A. S. Cacciapuoti.

Y. Sun and X. Dai are with the Key Laboratory of Wireless-Optical Communications, Chinese Academy of Sciences, School of Information Science and Technology, University of Science and Technology of China, Hefei 230026, China (e-mail: sys@mail.ustc.edu.cn; daixc@ustc.edu.cn).

Z. Ding is with the School of Electrical and Electronic Engineering, The University of Manchester, Manchester M13 9PL, U.K. (e-mail: zhiguo.ding@manchester.ac.uk).

G. K. Karagiannidis is with the Electrical and Computer Engineering Department, Aristotle University of Thessaloniki, 54124 Thessaloniki, Greece (e-mail: geokarag@auth.gr).

Color versions of one or more of the figures in this paper are available online at http://ieeexplore.ieee.org.

Digital Object Identifier 10.1109/TCOMM.2018.2825420

N-NOMA scheme, which combines SC with distributed analog beamforming is proposed. Specifically, SC is used to support a cell-edge user and users close to the BSs simultaneously, and distributed analog beamforming in order to improve the QoS of the cell-edge user. The reason for using distributed analog beamforming is twofold. On the one hand, analog beamforming modifies the signal's phase only, which means the BS only needs to know the phase of the channel. Thus, different BSs do not need to exchange instantaneous channel state information (CSI), and as a result, system overhead is reduced. On the other hand, due to the knowledge of the channel phase information, distributed analog beamforming can utilize the spatial degrees of freedom more efficiently than the space time block code (STBC) scheme used in [23], without using any CSI.

- Outage probability is used in this paper as the criterion to characterize the performance of the proposed scheme. The reason is that outage probability not only bounds the error probability of detection tightly, but also can be used to efficiently evaluate the outage sum rate/capacity. However, there are two obstacles to overcome in order to characterize the outage probability of the considered N-NOMA scheme, which makes the analysis very challenging: a) due to the combination of SC and distributed analog beamforming, the expression for the corresponding signal-to-interference-plus-noise ratio (SINR) is very different from those of the conventional communication schemes, b) how to capture the impact of the random users' locations on the performance of the considered N-NOMA scheme. By using rational approximations and rigorous derivations, the above difficulties can be perfectly settled, and closed-form analytical results of the outage probabilities achieved by the cell-edge user and near users are obtained.
- To get more insight into the proposed scheme, the impact of the system parameters, such as user locations, distances between BSs and power allocation coefficients, on the performance of the proposed N-NOMA, is discussed. For comparison purposes, a conventional OMA scheme, which uses distributed digital beamforming and serves only the cell-edge user, is considered. This comparison is facilitated, by using the analytical as well as the computer simulation results.

The rest of this paper is organized as follows. Section II illustrates the N-NOMA system model. Section III characterizes the outage performance of the proposed N-NOMA scheme. Section IV provides numerical results to demonstrate the performance of the proposed N-NOMA system and also verify the accuracy of the developed analytical results. Section V concludes the paper. Finally, Appendixes collect the proofs of the obtained analytical results.

II. System Model

Consider an N-NOMA downlink communication scenario, in which three BSs are supporting a cell-edge user cooperatively, while each BS is also individually communicating with a close user. More specifically, as shown in Fig. 1, consider an equilateral triangle, whose side length is denoted by l. Each BS, denoted by BS i, $1 \leq i \leq 3$, is located at one of the vertex of the equilateral triangle.[1] There is a big disc and a small disc centered at BS i, respectively. The big one is denoted by D_{0i}, and the small one by D_i. The locations of the users are described as follows. The cell-edge user is denoted by user 0 and its position (denoted by p_0) is assumed to be uniformly distributed in the intersecting area (which is denoted by A, and composed of three symmetrical areas, A_1, A_2 and A_3) of the three big discs. The user close to BS i is denoted by user i and its position (denoted by p_i) is assumed to be uniformly distributed in disc D_i. In addition, the size of the discs can be described as follows: the three big discs are assumed to have the same radius which is denoted by R_0; the radius of each small disc, i.e., D_i, $1 \leq i \leq 3$, is denoted by R_i. All the nodes in the considered scenario are equipped with a single antenna. Note that this paper focuses on sub-6 GHz networks, where the made single antenna assumption is reasonable in scenarios such as C-RAN and small cells, because BSs in such scenarios are usually limited in cost and size. Besides, considering multiple antennas equipped BSs will lead to other research challenges, such as how to group users or how to design beamformers, which are beyond the scope of this paper..

The reason for only considering two users for each BS in this paper is as follows. Pairing more than two users can enlarge the system throughput as shown in [7], however, this is at the expense of increasing the processing complexity of the SIC receiver. Thus, to reduce system complexity, pairing two users is more practical in NOMA systems and has been commenly considered in many existing NOMA studies. Moreover, the two-user pairing consideration is consistent with the specifications in 3GPP-LTE system [26].

A practical assumption about the range of R_0 is $\frac{\sqrt{3}}{3}l \leq R_0 \leq \frac{\sqrt{3}}{2}l$. The reasons for making this assumption are listed as follow. On the one hand, if R_0 is too small, the three big discs with radius R_0 have no intersecting area. On the other hand, if R_0 is too big, user 0 may be located too close to a BS, which contradicts with the assumption that user 0 is a cell edge user. Besides the above assumption for the big disc, the radius of each small disc should be carefully chosen to ensure that the cell-edge user is much further from the BS than the near users to apply NOMA.

The channel modeling used in this paper is described as follows. The channel gain between BS i and user j is modeled as $h_{ij} = g_{ij}/\sqrt{L_{ij}}$, where g_{ij} is the Rayleigh fading gain, i.e., $g_{ij} \sim CN(0,1)$, $L_{ij} = d_{ij}^{\alpha}$ denotes the path loss, d_{ij} is the distance between BS i and user j, and α is the path loss exponent parameter.

It is important to point out that, in the considered N-NOMA scheme, at the transmitter, BS i only needs to know the phase information of the channel between BS i and user 0, while at the receiver side, the users have the full CSI.

[1] Choosing three BSs represents a trade-off between performance and complexity. The use of the triangle based model provides convenience for the analysis. Although simple, this model will provide insights into the feasibility of the proposed N-NOMA scheme.

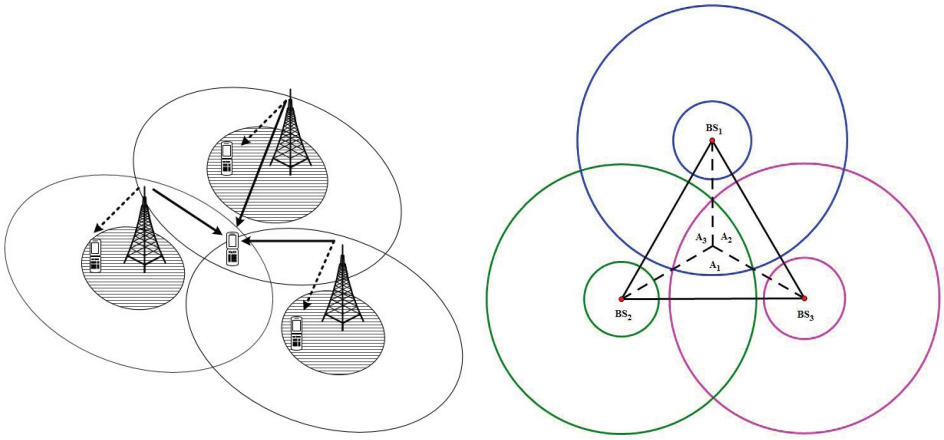

(a) (b)

Fig. 1. System model

BS i sends the following information[2]

$$x_i = \frac{h_{i0}^*}{|h_{i0}|}\beta_0\sqrt{P_s}s_0 + \frac{h_{i0}^*}{|h_{i0}|}\beta_1\sqrt{P_s}s_i, \quad (1)$$

where s_i, $0 \leq i \leq 3$, is the signal intended for user i, $E[|s_i|^2] = 1$, P_s is the transmit power, and β_0, β_1 are the power allocation coefficients with $\beta_0^2 + \beta_1^2 = 1$. In this paper, β_0 and β_1 are set to be constant and the same in all BSs. More sophisticated power allocation strategies can further improve the performance of the proposed N-NOMA system, but this is beyond the scope of this paper.

At the receiver side, the signal observed by user j, $0 \leq j \leq 3$, is given by

$$y_j = \sum_{i=1}^{3}\left(\frac{h_{i0}^* h_{ij}}{|h_{i0}|}\beta_0\sqrt{P_s}s_0 + \frac{h_{i0}^* h_{ij}}{|h_{i0}|}\beta_1\sqrt{P_s}s_i\right) + n_j, \quad (2)$$

where n_j is the noise observed at user j, and is modeled as a circular symmetric complex Gaussian random variable, i.e., $n_j \sim CN\left(0, \sigma^2\right)$, with σ^2 being the noise power.

One can note that the expression for the near user's received signal is different from that for the cell-edge's received signal. More specifically:

a) at user j, $1 \leq j \leq 3$, i.e., the near user, an interesting observation is that $\frac{h_{i0}^*}{|h_{i0}|}$ is uniformly distributed in $[0, 2\pi]$ and it is independent from h_{ij}. Thus $\frac{h_{i0}^*}{|h_{i0}|}h_{ij} \triangleq \tilde{h}_{ij}$ and h_{ij} are identically distributed, and then the received signal can be rewritten as

$$y_j = \sum_{i=1}^{3}\left(\tilde{h}_{ij}\beta_0\sqrt{P_s}s_0 + \tilde{h}_{ij}\beta_1\sqrt{P_s}s_i\right) + n_j, j = 1, 2, 3. \quad (3)$$

According to the NOMA principle, user j, $1 \leq j \leq 3$, carries out successive interference cancellation (SIC) by first removing the message to user 0 with

$$\text{SINR}_{j,0} = \frac{\left|\sum_{i=1}^{3}\tilde{h}_{ij}\right|^2\beta_0^2}{\sum_{i=1}^{3}\left|\tilde{h}_{ij}\right|^2\beta_1^2 + 1/\rho}, \quad (4)$$

where $\rho = P_s/\sigma^2$ is the transmit signal-to-noise ratio (SNR). If successful, user j then decodes its own message with

$$\text{SINR}_j = \frac{\left|\tilde{h}_{jj}\right|^2\beta_1^2}{\sum_{\substack{i=1\\ i\neq j}}^{3}|\tilde{h}_{ij}|^2\beta_1^2 + 1/\rho}. \quad (5)$$

b) at user 0, i.e.,the cell-edge user, the received signal can be expressed as

$$y_0 = \sum_{i=1}^{3}\left(|h_{i0}|\beta_0\sqrt{P_s}s_0 + |h_{i0}|\beta_1\sqrt{P_s}s_i\right) + n_0. \quad (6)$$

In order to decode the received message, user 0 treats s_i, $1 \leq i \leq 3$, as additive noise, which means that user 0 decodes its message with

$$\text{SINR}_0 = \frac{\left(\sum_{i=1}^{3}|h_{i0}|\right)^2\beta_0^2}{\sum_{i=1}^{3}|h_{i0}|^2\beta_1^2 + 1/\rho}. \quad (7)$$

The proposed N-NOMA scheme can deal with the scenario with multiple cell-edge users by allocating these cell-edge users different orthogonal resource blocks. In each resource block, a cell-edge user and near users are grouped and served simultaneously by the proposed N-NOMA. If there are more than one cell-edge users in each orthogonal resource block, then the round-robin method can be applied. This method is referred to as hybrid N-NOMA, since both OMA and NOMA are used.

For comparison purposes, the following benchmark scheme, based on conventional OMA, is considered. This scheme only

[2]Note that, the cell-edge user is far from the BSs and ensuring the cell-edge user's Qos is most important, thus the BSs coordinate to serve the cell-edge user. For system simplicity, it is assumed that there is no coordination for near users.

serves the cell-edge user by using the same channel resource block as the above N-NOMA scheme. Distributed digital beamforming is employed, i.e., the transmit signal at each BS is given by $\tilde{x}_i = \frac{h_{i0}^*}{\sqrt{\sum_{i=1}^{3}|h_{i0}|^2}}\sqrt{3P_s}s_0$. Note that, the overall transmit power of the three BSs is $3P_s$, which is the same as the proposed N-NOMA scheme. It is also important to point out that, in the benchmark OMA scheme, all the nodes have access to the full CSI.

III. Performance Analysis

In this section, we use the outage probability as the criterion to characterize the performance of the proposed N-NOMA scheme. Meanwhile, the outage probability achieved by the benchmark scheme is also obtained by considering the impact of the random location of the cell-edge user. It should be pointed out that throughout the paper, the signals intended for different users are independently coded with Gaussian codebooks to achieve the Shannon capacity.

A. Outage Performance at User 0

The outage probability for user 0 to decode its information is given by

$$P_0 = P\left(\frac{\left(\sum_{i=1}^{3}|h_{i0}|\right)^2\beta_0^2}{\sum_{i=1}^{3}|h_{i0}|^2\beta_1^2+1/\rho} < \eta_0\right), \tag{8}$$

where $\eta_j = 2^{r_j}-1$ and r_j is the target data rate of user j, $0 \le j \le 3$. It is worth rewriting P_0 as

$$P_0 = P\Big(\left(\beta_0^2-\beta_1^2\eta_0\right)\left(|h_{10}|^2+|h_{20}|^2+|h_{30}|^2\right) +2\beta_0^2\left(|h_{10}||h_{20}|+|h_{10}||h_{30}|+|h_{20}||h_{30}|\right) < \frac{\eta_0}{\rho}\Big). \tag{9}$$

As it can be seen in (9), the outage probability achieved by user 0 can be less than 1, even when $\beta_0^2-\beta_1^2\eta_0 \le 0$. But, in this paper, we assume that $\beta_0^2-\beta_1^2\eta_0 > 0$. The reason for making this assumption is that, when $\beta_0^2-\beta_1^2\eta_0 \le 0$, the outage probabilities achieved by user 1, 2 and 3 will always be 1. Under this assumption, it is not hard to find the impact of l and β_1 on the outage performance of user 0 as shown in the following propositions.

Proposition 1: The outage probability achieved by user 0 *is a monotonically increasing function with respect to* l *(i.e.,the distance between the BSs), when* β_0, η_0, ρ *and* k *are fixed.*

Proposition 2: The outage probability achieved by user 0 *is a monotonically increasing function of* β_1*, which is the power allocation coefficient corresponding to the near user.*

The following lemma, which provides a closed-form expression for P_0, is presented.

Lemma 1: In the high SNR regime, the outage probability at user 0 *can be approximated in closed-form as*

$$P_0 \approx \underbrace{\frac{4\left(G(\phi)-F(\phi)+F(0)\right)}{\left(\beta_0^2-\beta_1^2\eta_0\right)^2}}_{\kappa(\beta_0,\beta_1,\eta_0,\rho)} E_{p_0}\left\{L_{10}L_{20}L_{30}\right\}, \tag{10}$$

where $\phi = \sqrt{\frac{\eta_0}{\rho(2\beta_0^2-\beta_1^2\eta_0)}}$*, the functions* $F(v)$ *and* $G(v)$ *are defined as shown in (12), as shown at the bottom of the next page, in (12),* a, b, c *and* d *are used to simplify the expression and are given by*

$$\begin{cases} a = \beta_0^2\beta_1^2\eta_0 - \beta_1^4\eta_0^2 \\ b = 3\beta_0^2\beta_1^2\eta_0 - \beta_1^4\eta_0^2 \\ c = (\beta_0^2-\beta_1^2\eta_0)\eta_0/\rho \\ d = 2\beta_0^4 + 3\beta_0^2\beta_1^2\eta_0 - \beta_1^4\eta_0^2 \\ \phi = \sqrt{\frac{\eta_0}{\rho(2\beta_0^2-\beta_1^2\eta_0)}}, \end{cases}$$

and $E_{p_0}\{L_{10}L_{20}L_{30}\}$*, is the expectation of the product of* L_{10}*,* L_{20} *and* L_{30} *with respect to* p_0*, when* $\alpha = 2$*,* $E_{p_0}\{L_{10}L_{20}L_{30}\}$ *can be expressed as shown in (11), as shown at the bottom of the next page, in (11),* S_A *is the area of* A*, and can be expressed as*

$$S_A = 3R_0^2\left(\frac{\pi}{3}-\arcsin\left(\frac{l}{2R_0}\right)\right) -\sqrt{3}lR_0\sin\left(\frac{\pi}{3}-\arcsin\left(\frac{l}{2R_0}\right)\right), \tag{13}$$

when $\alpha > 2$*,* $E_{p_0}\{L_{10}L_{20}L_{30}\}$ *is approximated by considering the special case when user* 0 *is located very close to the center of the equilateral triangle and given by*

$$E_{p_0}\{L_{10}L_{20}L_{30}\} \approx 3^{-\frac{3\alpha}{2}}l^{3\alpha}. \tag{14}$$

Proof: Please refer to Appendix A. ∎

Remark 1: The main difficulties to get P_0 *are listed as follows: firstly, the distributions of* $|h_{i0}|$ *are correlated because* $|h_{i0}|$ *is revelent to the location of user* 0*. Secondly, in (9), the left hand side of the inequality contains product terms. As can be seen in Appendix A, by considering the high SNR regime, the mentioned two difficulties be can be solved separately for analysis simplification.*

As shown in Lemma 1, the first part of the expression for P_0, $\kappa(\beta_0,\beta_1,\eta_0,\rho)$, is a function of β_0,β_1,η_0 and ρ, while the second part, $E_{p_0}\{L_{10}L_{20}L_{30}\}$, is a function of l and R_0. By further analyzing $\kappa(\beta_0,\beta_1,\eta_0,\rho)$, it is not hard to conclude that the diversity obtained by user 0 is 3, since there is a common factor $1/\rho^3$.

To get insight into the impact of R_0 on P_0, we focus on the case when $\alpha = 2$. Note that, (11) can be rewritten as

$$E_{p_0}\{L_{10}L_{20}L_{30}\} = \lambda(k)l^6, \tag{15}$$

where $k = \frac{R_0}{l}$, and $\lambda(k)$ is a function of k, which can be expressed as shown in (16), as shown at the bottom of the next page.

The simulation results shown in Fig. 2 indicate that $\lambda(k)$ is a monotonically decreasing function of k in the interval of $\frac{\sqrt{3}}{3} \le k \le \frac{\sqrt{3}}{2}$, although we cannot find a formal proof for this yet. Thus we highlight the following remark.

Remark 2: In the high SNR regime, the outage probability achieved by user 0 *is a monotonically decreasing function with respect to* k *(or* R_0*), when* β_0, η_0, ρ *and* l *are fixed.*

It is also interesting to consider the special case when user 0 is located very close to O. Fig. 2 indicates that, when k

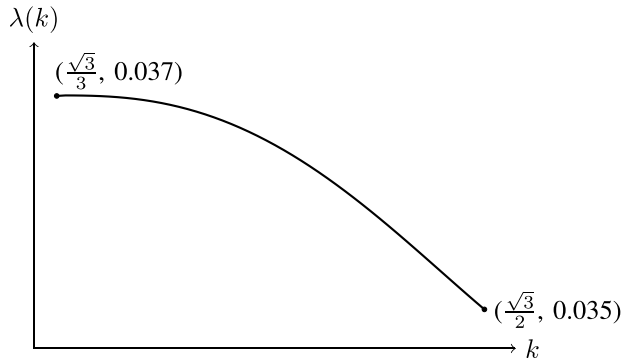

Fig. 2. Illustration of function $\lambda(k)$.

approaches $\frac{\sqrt{3}}{3}$ from the right-hand side, the slope of the curve is nearly 0. Thus when user 0 is located very close to O, the impact of different choices of R_0 on P_0 is negligible, this observation is consistent with the expression (14) presented in Lemma 1, where R_0 is neglected.

1) The case of the Benchmark Network OMA Scheme: To facilitate comparison, we also consider the special case when user 0 is located very close to O for the benchmark OMA scheme. The following lemma characterize the outage performance of the benchmark OMA scheme:

Lemma 2: In the scenario where user 0 *is located very close to O, the outage probability achieved by user* 0 *over the benchmark OMA scheme can be approxiamted as follows:*

$$\tilde{P}_0 \approx \frac{e^{-\frac{3^{-\frac{\alpha}{2}-1}\eta_0 l^\alpha}{\rho}}}{2\times 3^{\alpha+2}\rho^2}\times\left(-\eta_0^2 l^{2\alpha}+2\times 3^{\alpha+2}\rho^2\left(e^{\frac{3^{-\frac{\alpha}{2}-1}\eta_0 l^\alpha}{\rho}}-1\right)-2\times 3^{\frac{\alpha}{2}+1}\eta_0\rho l^\alpha\right). \quad (17)$$

Proof: Please refer to Appendix B. ■

B. Outage Performance at User j, $1 \le j \le 3$, Achieved by N-NOMA

The QoS requirement of user j can be met only when the following two constraints are satisfied: a) user j can decode the message intended to user 0, and b) user j can decode its own message after successfully removing the message intended to user 0. More rigorously, we define the outage events at user j as follows. First define, $E_{j,k} \triangleq \{\text{SINR}_{j,k} < \eta_k\}$, as the event that user j cannot decode the message intended to user k, where $1 \le j \le 3$, $k \in \{0, j\}$, and $E_{j,k}^c$ as the complementary set of $E_{j,k}$. Thus the outage probability at user j can be expressed as

$$P_j = 1 - P(E_{j,0}^c \cap E_{j,j}^c) = P(E_{j,0} \cup E_{j,j}). \quad (18)$$

In order to reduce the complexity of the performance analysis, it is important to note that, when $l >> R_j$, $\tilde{h}_{ij}$ $(i \ne j)$ is much smaller than $\tilde{h}_{jj}$ because of large scale propagation losses. Thus the SINR to decode s_0 at user j, $1 \le j \le 3$, can be approximated as

$$\text{SINR}_{j0} \approx \frac{\left|\tilde{h}_{jj}\right|^2 \beta_0^2}{\sum_{i=1}^{3}\left|\tilde{h}_{ij}\right|^2 \beta_1^2 + 1/\rho}. \quad (19)$$

This assumption is reasonable, since in realistic systems, the distances between the BSs are usually much further than that between a BS and its near user. Following this approximation, $E_{j,0}$ can be expressed as

$$E_{j,0} = \left\{\left|\tilde{h}_{jj}\right|^2 < \frac{\eta_0}{\beta_0^2 - \beta_1^2\eta_0}\left(\sum_{\substack{i=1\\ i\ne j}}^{3}\left|\tilde{h}_{ij}\right|^2\beta_1^2 + 1/\rho\right)\right\}. \quad (20)$$

$$E_{p_0}\{L_{10}L_{20}L_{30}\} = \frac{1}{8S_A}\left(\frac{l^8}{8\sqrt{3}} + \left(3\sqrt{3}+4\pi\right)l^4R_0^4 + 8\left(\sqrt{3}+\pi\right)l^2R_0^6 + 2\pi R_0^8 - 6R_0^4\left(2l^4+4l^2R_0^2+R_0^4\right)\sin^{-1}\left(\frac{l}{2R_0}\right) - \frac{1}{8}lR_0\sqrt{4-\frac{l^2}{R_0^2}}\left(l^6+2l^4R_0^2+102l^2R_0^4+84R_0^6\right)\right). \quad (11)$$

$$\begin{cases} F(v) = \frac{2\sqrt{2}\beta_0^2}{48a^{3/2}}\left(-\frac{c^3(2a-b)\tanh^{-1}\left(\frac{\sqrt{a}v}{\sqrt{(a+b)v^2+c}}\right)}{b^2} - \frac{\sqrt{a}v\sqrt{(a+b)v^2+c}\left(b(b-2a)v^4+2bcv^2+c^2\right)}{b} \right. \\ \qquad + v^2\left(b(4a+b)v^4+3(2a+b)cv^2+3c^2\right)\log\left(\frac{\sqrt{v^2(a+b)+c}+\sqrt{a}v}{\sqrt{bv^2+c}}\right) \\ \qquad \left. + \frac{2a^{3/2}c^3\log\left(\sqrt{a+b}\sqrt{(a+b)v^2+c}+av+bv\right)}{b^2\sqrt{a+b}}\right) \\ G(v) = \frac{2}{15}\left(\frac{av^6}{6}+\frac{5cv^4}{4}+\frac{5dv^6}{6}\right), \end{cases} \quad (12)$$

$$\lambda(k) = \frac{1}{192k\left(\pi k - 3k\sin^{-1}\left(\frac{1}{2k}\right) - \sqrt{3}\cos\left(\sin^{-1}\left(\frac{1}{2k}\right)+\frac{\pi}{6}\right)\right)}\times\left(48\pi k^8 - 3\sqrt{4-\frac{1}{k^2}}\left(84k^6+102k^4+2k^2+1\right)k + \sqrt{3} + 192\left(\sqrt{3}+\pi\right)k^6 + 24\left(3\sqrt{3}+4\pi\right)k^4 - 144\left(k^4+4k^2+2\right)k^4\sin^{-1}\left(\frac{1}{2k}\right)\right). \quad (16)$$

It is important to point out that the assumption $\beta_0^2 - \beta_1^2\eta_0 > 0$ is applied in the above expression. Since if $\beta_0^2 - \beta_1^2\eta_0 \leq 0$, P_j will always be 1. Using the same format as in (20), $E_{j,j}$ can be expressed as

$$E_{j,j} = \left\{ \left|\tilde{h}_{jj}\right|^2 < \frac{\eta_j}{\beta_1^2}\left(\sum_{\substack{i=1\\ i\neq j}}^{3}\left|\tilde{h}_{ij}\right|^2\beta_1^2 + 1/\rho\right)\right\}. \quad (21)$$

Therefore the outage probability achieved by user j can be further formulated as

$$P_j = P\left(\left|\tilde{h}_{jj}\right|^2 < M_j\left(\sum_{\substack{i=1\\ i\neq j}}^{3}\left|\tilde{h}_{ij}\right|^2\beta_1^2 + 1/\rho\right)\right), \quad (22)$$

where $M_j = \max\left\{\frac{\eta_0}{\beta_0^2-\beta_1^2\eta_0}, \frac{\eta_j}{\beta_1^2}\right\}$. The following lemma characterizes the outage performance at user j, $1 \leq j \leq 3$.

Lemma 3: When $l >> R_j$, then the outage probability achieved by user j, $1 \leq j \leq 3$, can be approximated as

$$P_j \approx 1 - \frac{2\rho^{\frac{2}{\alpha}} M_j \gamma(\frac{2}{\alpha}, \frac{M_j R_j^\alpha}{\rho}) - \frac{4\beta_1^2 M_j \rho^{\frac{2}{\alpha}+1}}{l^\alpha}\gamma(\frac{2}{\alpha}+1, \frac{M_j R_j^\alpha}{\rho})}{\alpha M_j^{\frac{2}{\alpha}+1} R_j^2}. \quad (23)$$

where $\gamma(s,x)$ is the the lower incomplete gamma function defined as $\gamma(s,x) = \int_0^x t^{s-1}e^{-t}\,\mathrm{d}t$.

Proof: Please refer to Appendix C. ∎

By using Lemma 3, the following corollaries can be obtained to show how system parameters, β_1, l and R_j, affect the outage performance, achieved by user j.

Corollary 1: When $l >> R_j$, then the outage probability at high SNR achieved by user j, $1 \leq j \leq 3$, is a monotonically increasing function of R_j.

Proof: Here, we concentrate on the case when $\alpha = 2$. Note that, from (23), for $\alpha = 2$, P_j can be approximated as

$$P_j \approx 1 - \frac{\rho e^{-\frac{M_j R_j^2}{\rho}}}{l^2 M_j R_j^2}\left(l^2\left(e^{\frac{M_j R_j^2}{\rho}} - 1\right) + 2\beta_1^2\left(-\rho e^{\frac{M_j R_j^2}{\rho}} + M_j R_j^2 + \rho\right)\right). \quad (24)$$

Note that, the partial derivative of R_j^2 for P_j is

$$\frac{\partial P_j}{\partial R_j^2} = \frac{M_j\left(3l^2 + 2\beta_1^2\left(3\rho - 4M_j R_j^2\right)\right)}{6l^2\rho}. \quad (25)$$

Note that $l >> R_j$, thus $\frac{\partial P_j}{\partial R_j^2} > 0$ and the proof is completed. ∎

Corollary 2: When $l >> R_j$, then

1) *if $0 < \beta_1^2 \leq \frac{\eta_j}{\eta_0+\eta_j+\eta_0\eta_j}$, the outage probability achieved by user j, $1 \leq j \leq 3$, is a monotonically decreasing function of β_1^2,*
2) *if $\frac{\eta_j}{\eta_0+\eta_j+\eta_0\eta_j} < \beta_1^2 < \frac{1}{1+\eta_0}$, the outage probability achieved by user j, $1 \leq j \leq 3$, is a monotonically increasing function of β_1^2.*

Proof:

1) When $0 < \beta_1^2 \leq \frac{\eta_j}{\eta_0+\eta_j+\eta_0\eta_j}$ and $M_j = \frac{\eta_j}{\beta_1^2}$, P_j can be expressed as

$$P_j = P\left(\left|\tilde{h}_{jj}\right|^2 < \frac{\eta_j}{\beta_1^2}\left(\sum_{\substack{i=1\\ i\neq j}}^{3}\left|\tilde{h}_{ij}\right|^2\beta_1^2 + 1/\rho\right)\right). \quad (26)$$

Note that $\frac{\eta_j}{\beta_1^2}\left(\sum_{\substack{i=1\\ i\neq j}}^{3}\left|\tilde{h}_{ij}\right|^2\beta_1^2 + 1/\rho\right)$ in (22) is a monotonically decreasing function of β_1^2, thus P_j is also a monotonically decreasing function of β_1^2.

2) When $\frac{\eta_j}{\eta_0+\eta_j+\eta_0\eta_j} < \beta_1^2 < \frac{1}{1+\eta_0}$ and $M_j = \frac{\eta_0}{\beta_0^2-\beta_1^2\eta_0}$, P_j can be expressed as

$$P_j = P\left(\left|\tilde{h}_{jj}\right|^2 < \frac{\eta_0}{\beta_0^2 - \beta_1^2\eta_0}\left(\sum_{\substack{i=1\\ i\neq j}}^{3}\left|\tilde{h}_{ij}\right|^2\beta_1^2 + 1/\rho\right)\right). \quad (27)$$

Note that $\frac{\eta_0}{\beta_0^2-\beta_1^2\eta_0}\left(\sum_{\substack{i=1\\ i\neq j}}^{3}\left|\tilde{h}_{ij}\right|^2\beta_1^2 + 1/\rho\right)$ in (22) is a monotonically increasing function of β_1^2, thus P_j is also a monotonically increasing function of β_1^2.

∎

C. Outage Performance at User j, $1 \leq j \leq 3$, Achieved by N-NOMA With Co-Channel Interference

Until now, the outage performance of the cell-edge user and the near users are analyzed by ignoring the co-channel interference outside the considered three BSs. However, in a practical system, the considered users receive signals not only from the mentioned BSs, but also from co-channel interference sources, hence, it is essential to consider the case with co-channel interference. In this paper, we model the interference sources as a homogeneous Poisson point process Φ_I with intensity λ_I, i.e., $\Phi_I = \{p_{I_k}\}$, where p_{I_k} is the location of the k-th interference source. For tractable analysis, it is assumed that the interference sources use identical transmission powers, denoted by P_I.

Under the above interference model, the signal observed by user j, $0 \leq j \leq 3$, is now expressed as:

$$y_j = \sum_{i=1}^{3}\left(\frac{h_{i0}^* h_{ij}}{|h_{i0}|}\beta_0\sqrt{P_s}s_0 + \frac{h_{i0}^* h_{ij}}{|h_{i0}|}\beta_1\sqrt{P_s}s_i\right) + \omega_{I_j} + n_j, \quad (28)$$

where ω_{I_j} is the overall co-channel interference observed by user j, and can be expressed as follows:

$$\omega_{I_j} \triangleq \sum_{p_{I_k}\in\Phi_I}\frac{g_{I_k,j}}{\sqrt{L(d_{I_k,j})}}\sqrt{P_I}\tilde{s}_{I_k} \quad (29)$$

where $\tilde{s}_{I_k}$ is the normalized signal sent by the k-th interference source, i.e., $E[|\tilde{s}_{I_k}|^2] = 1$, and these signals are assumed to

be independent from each other. $d_{I_k,j}$ is the distance between user j and the k-th interference source, and $g_{I_k,j}$ is the corresponding Rayleigh fading gain, i.e., $g_{I_k,j} \sim CN(0,1)$.

After considering the case with co-channel interference, the outage probabilities expressed in (8) and (22) become

$$P_0^{\text{Inter}} = P\left(\frac{\left(\sum_{i=1}^{3}|h_{i0}|\right)^2 \beta_0^2}{\sum_{i=1}^{3}|h_{i0}|^2\beta_1^2 + I_0 + 1/\rho} < \eta_0\right), \quad (30)$$

for the cell-edge user and

$$P_j^{\text{Inter}} = P\left(\left|\tilde{h}_{jj}\right|^2 < M_j\left(\sum_{\substack{i=1\\ i\neq j}}^{3}\left|\tilde{h}_{ij}\right|^2\beta_1^2 + I_j + 1/\rho\right)\right), \quad (31)$$

for near users $(1 \le j \le 3)$, where $I_j = \sum_{p_{I_k}\in\Phi_I} \frac{|g_{I_k,j}|^2}{L(d_{I_k,j})}\rho_I, 0 \le j \le 3$, where $\rho_I = \frac{P_I}{P_s}$. Analyzing the outage probability in (30) is very difficult, thus we focus on analyzing the outage probability for the near users. Thanks to stochastic geometry, we get the following lemma to characterize the outage performance of the near users in the case with co-channel interference.

Lemma 4: When $l >> R_j$, then the outage probability achieved by user j, $1 \le j \le 3$, can be approximated as

$$P_j^{Inter} \approx \sum_{n=1}^{N}\frac{\pi}{NR_j}\sqrt{1-\theta_n^2}f\left(\frac{R_j}{2}\theta_n + \frac{R_j}{2}\right), \quad (32)$$

where N denotes the parameter for Gauss-Chebyshev quadrature, $\theta_n = \cos\frac{(2n-1)\pi}{2N}$ and

$$f(x) = (x - \frac{2\beta_1^2 M_j}{l^\alpha}x^{\alpha+1}) \times \exp\left(-\frac{M_j}{\rho}x^\alpha - 2\pi\lambda_I\frac{(M_j\rho_I)^{\frac{2}{\alpha}}}{\alpha}B\left(\frac{2}{\alpha}, 1-\frac{2}{\alpha}\right)x^2\right), \quad (33)$$

where $B(\cdot)$ is the Beta function.

Proof: Please refer to Appendix D. ■

IV. Numerical Results and Simulations

In this section, computer simulations are performed to demonstrate the performance of the proposed N-NOMA system and also verify the accuracy of the analytical results. The thermal noise power is set as -170 dBm/Hz, the carrier frequency is 2×10^9 Hz, the transmission bandwidth is 10 MHz, and the transmitter and receiver antenna gain are set as 1.

Fig. 3 and Fig. 4 shows a performance comparison of the proposed N-NOMA scheme and the conventional OMA scheme. In Fig. 3(a), the outage sum rates are shown as functions of the transmission power, the corresponding outage probabilities are shown in Fig. 3(b). Note that, when using the N-NOMA, the cell-edge user may have some rate loss compared to the conventional OMA, this rate loss is quantified

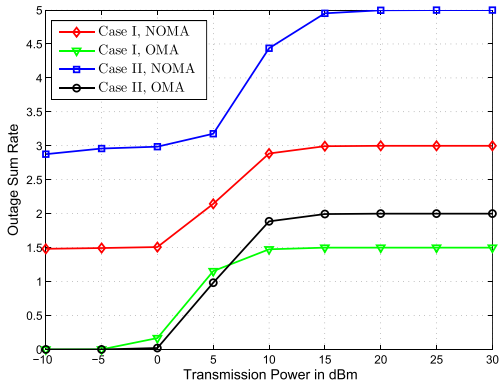

(a) Outage Sum Rate

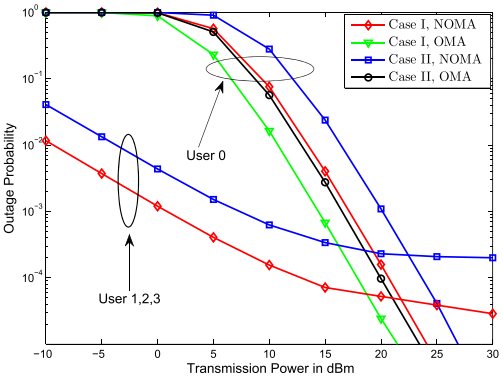

(b) Outage Probability

Fig. 3. Performance comparison of N-NOMA and conventional OMA. Case I: $r_0 = 1.5$ BPCU, $r_1 = r_2 = r_3 = 0.5$ BPCU. Case II: $r_0 = 2$ BPCU, $r_1 = r_2 = r_3 = 1$ BPCU.

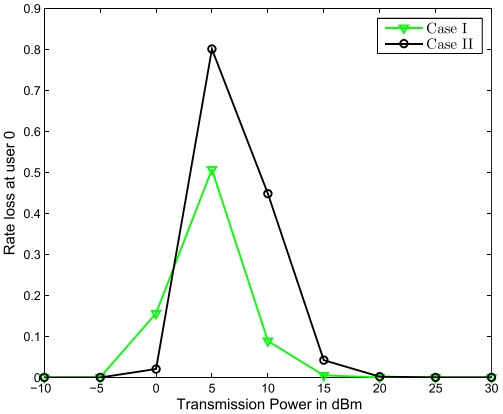

Fig. 4. Rate loss at the cell-edge user. Case I: $r_0 = 1.5$ BPCU, $r_1 = r_2 = r_3 = 0.5$ BPCU. Case II: $r_0 = 2$ BPCU, $r_1 = r_2 = r_3 = 1$ BPCU.

as shown in Fig. 4. The parameters are set as: $l = 400m$, $R_0 = 250m$, $R_j = 10m, 1 \le j \le 3$, $\beta_0^2 = \frac{4}{5}, \alpha = 3$. Fig. 3(b) shows that, at user 0, the outage probability achieved by the conventional OMA is lower than that achieved by the considered N-NOMA. The reason is that, the conventional OMA scheme serves only the cell-edge user and digital beamforming is superior to analog beamforming. But, as it can be seen from Fig. 3(a) and Fig. 4, with some tolerable rate loss at the cell edge user, the proposed N-NOMA scheme can achieve a higher outage sum rate, compared to the conventional OMA,

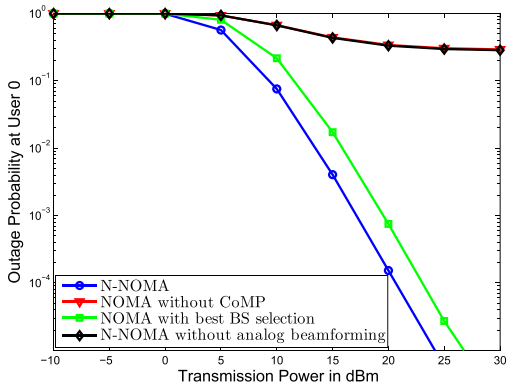

Fig. 5. Comparison of N-NOMA with other three benchmark NOMA schemes.

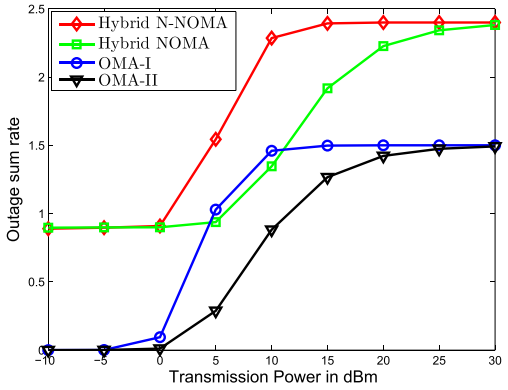

Fig. 6. Comparison of hybrid N-NOMA with other three benchmarks.

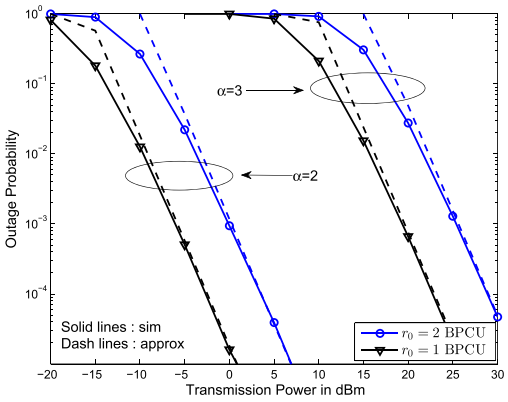

Fig. 7. Outage performance at user 0 for the N-NOMA system. $l = 600m$, $R_0 = 400m$.

which demonstrates the superior special efficiency of NOMA. For example, as shown in Fig. 3(a), in Case II, when the transmit power is 30 dBm, the sum rate achieved by the proposed N-NOMA is about 5 bits per channel use (BPCU), while that of the conventional OMA scheme is about 2 BPCU. Hence the gap is about 3 BPCU.

Fig. 5 shows a performance comparison of the proposed N-NOMA scheme with other three benchmark NOMA schemes, named NOMA without CoMP, NOMA with best BS selection and N-NOMA without analog beamforming, respectively. In NOMA without CoMP and NOMA with best BS selection, only one BS, employs NOMA to support the cell-edge user and its near user, which means, the transmit signals are as follows: $x_1 = \beta_0\sqrt{3P_s}s_0 + \beta_1\sqrt{P_s}s_1$ and $x_j = \beta\sqrt{P_s}s_j, j = 2, 3$. The difference between NOMA without CoMP and NOMA with best BS selection is as follows: i) in NOMA without CoMP scheme, the BS which serves the cell-edge user is randomly chosen from the three BSs, ii) in NOMA with best BS selection scheme, the BS with the largest channel gain, i.e., $|h_{i0}|^2$, is chosen. Note that, the transmission power for user 0 becomes $3\beta_0^2 P_s$ in the two benchmark NOMA schemes, which may be impractical because the transmission power at BS 1 may excess the power constraint. Even so, as shown in Fig. 5, the outage performance at user 0 achieved by N-NOMA is much better than that of the two benchmark NOMA schemes. In N-NOMA without analog beamforming, the message sent by BS j is $x_j = \beta_0\sqrt{P_s}s_0 + \beta_1\sqrt{P_s}s_j, j = 1, 2, 3$. As can be seen in the figure, the performance of N-NOMA without analog beamforming is much worse than that of the proposed N-NOMA scheme. The above observation indicates the importance of applying diversity techniques when serving the cell-edge user.

Fig. 6 shows the comparison of the hybrid N-NOMA scheme with other benchmarks in the scenario with three cell-edge users. For the four schemes presented in the figure, the transmission time interval is divided into three time slots, i.e., each cell-edge user is assigned a time slot. More specifically, in the OMA-I scheme, the three BSs apply analog beamforming to cooperatively serve a cell-edge in a time slot, while in the OMA-II scheme, a cell-edge user is served by only a single BS. Different from the two OMA schemes, the two NOMA schemes serve one cell-edge user and the near users simultaneously in a time slot. Particularly, in the hybrid N-NOMA scheme, the three BSs apply the proposed N-NOMA to serve a cell-edge user and their associated near users simultaneously in a time slot. While in the hybrid NOMA scheme, a cell-edge user is associated with a single BS, which means each BS serves a cell-edge user and its near user simultaneously in a time slot. Note that, to facilitate the comparison, the total transmission powers of all the schemes are assumed to be the same. The target date rate for each cell-edge user is 0.5 BPCU and the rate for each near user is 0.3 BPCU. From the figure, it is clear that hybrid N-NOMA outperforms other three schemes. Furthermore, the comparison between the hybrid N-NOMA scheme and the hybrid NOMA scheme indicates the importance for applying diversity techniques. Meanwhile, the comparison between the hybrid N-NOMA scheme with OMA-I demonstrates the superiority of NOMA compared to OMA, since NOMA exploits the channel differences between the users.

In Fig. 7 and Fig. 8, the accuracy of the analytical results developed in Lemma 1 are verified. The power allocation coefficient is set as: $\beta_0^2 = \frac{4}{5}$. As it is evident from Fig. 7 and Fig. 8, the approximation results of Lemma 1 are accurate in the high SNR regime. It is also verified in Fig. 8 that P_0 increases with l.

In Fig. 9, the accuracy of the analytical results developed in Lemma 3 and Lemma 4 are verified. The parameters are set as: $l = 300m$, $R_0 = 200m$, $R_j = 20m, 1 \le j \le 3$, $\beta_0^2 = \frac{4}{5}$, $\lambda_I = \frac{1}{\pi 200^2}$, $\alpha = 4$, and $r_j = 0.5$ BPCU, $0 \le j \le 3$. Note that,

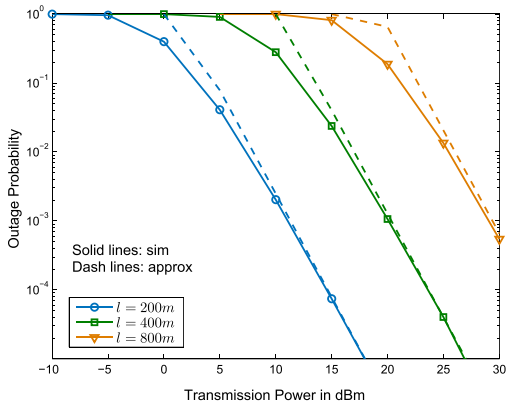

Fig. 8. Impact of l on P_0. $\alpha = 3$, $R_0 = \frac{11}{10} \times \frac{l}{\sqrt{3}}$, $r_0 = 2$ BPCU.

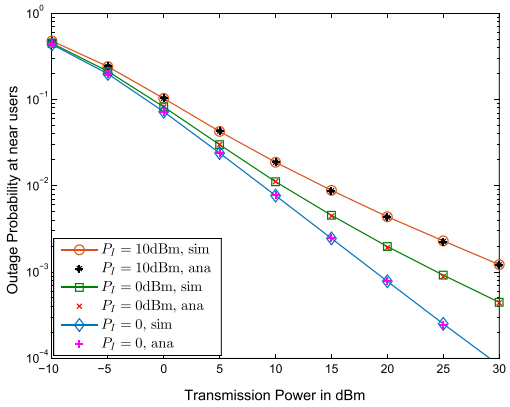

Fig. 9. Outage performance at near users.

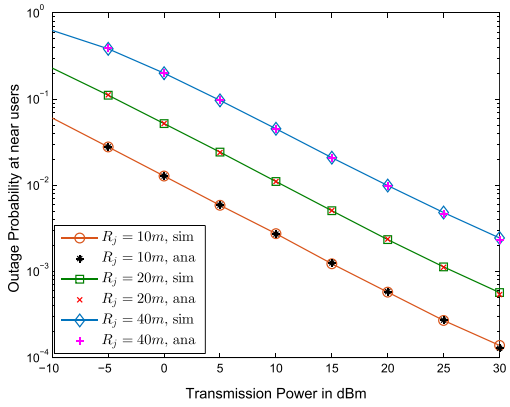

Fig. 10. Impact of the distance between a BS and its near user on the outage probability at the near user. $1 \leq j \leq 3$.

for the interference free case, i.e., $P_I = 0$, the analytical results are based on Lemma 3, while for $P_I > 0$, the analytical results are based on Lemma 4. As shown in the figure, the simulations perfectly matches the analytical results, thus the validity of the analysis based on the assumption that $l >> R_j$ is verified. It is also evident, as shown in the figure, as the interference power increases, the outage performance of the near users becomes worse, which is consistent with our intuition.

In Fig. 10, the impact of the distance between a BS and its near user on the outage probability achieved by the near user is investigated. The parameters are set as: $l = 400$m, $R_0 = 250$m, $r_j = 0.5$ BPCU, $0 \leq j \leq 3$, $P_I = 6$dBm, $\lambda_I = \frac{1}{\pi 200^2}$, $\beta_0^2 = \frac{4}{5}$ and $\alpha = 3$. As it also concluded from this figure, given a fixed transmission power, the outage probability achieved by the near user is increased after an increase of the distance between the BS and its near user. This is reasonable, because as the distance between a BS and its near user increases, the large scale propagation losses become severe.

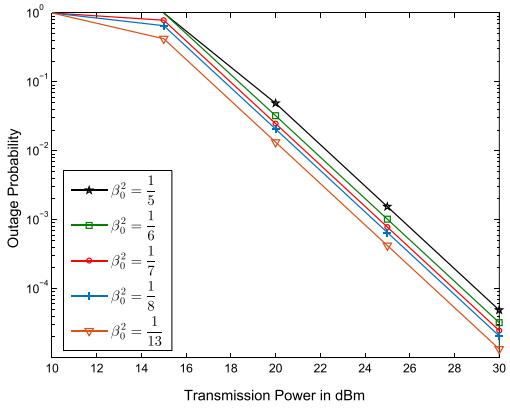

(a) User 0

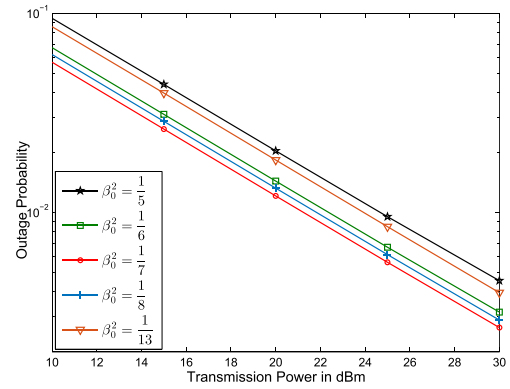

(b) User 1, 2 and 3

Fig. 11. Impact of power allocation coefficients on the outage probability.

In Fig. 11, the impact of the power allocation coefficients on the outage probability is studied. The parameters are set as: $l = 600m$, $R_0 = 400m$, $R_j = 30m, 1 \leq j \leq 3$, $r_0 = 2$ BPCU, $r_1 = r_2 = r_3 = 1$ BPCU, $P_I = 6$dBm, $\lambda_I = \frac{1}{\pi 200^2}$ and $\alpha = 3$. As it can be seen from Fig. 11(a), the outage probability achieved by user 0 increases with β_1. Fig. 11(b) shows that, when $\beta_1^2 < \frac{\eta_j}{\eta_0 + \eta_j + \eta_0 \eta_j} = \frac{1}{7}$, the outage probabilities achieved by user 1, 2 and 3 decrease with β_1. On the other hand, when $\beta_1^2 > \frac{1}{7}$, the outage probabilities achieved by user 1, 2 and 3 increase with β_1. Thus the simulation results comfirm the conclusions presented in Proposition 2 and Corollary 2.

V. Conclusion

In this paper, in order to show the feasibility of N-NOMA, we have proposed a distributed analog beamforming based N-NOMA scheme for a downlink CoMP system with

randomly deployed users. Closed-form analysis of the outage probability, achieved by the proposed transmission scheme, has been developed to facilitate the performance evaluation. The impact of system parameters, such as user locations, distances between BSs and power allocation coefficients, on the outage performance has also been captured. Computer simulation results have been provided to demonstrate the accuracy of the developed analytical results. The proposed N-NOMA outperforms conventional OMA scheme, as demonstrated by the presented analytical and computer simulation results. Note that, fixed power allocation coefficients are used in this paper, and it is important to study more sophisticated power allocation strategies in order to improve the performance of N-NOMA in the future.

For a general system model with more BSs, stochastic geometry can be applied. More specifically, a poisson cluster point process (PCP) can be considered as in [27]. Particularly, the locations of the base stations $\{x_i\}$ are modelled as a parent homogeneous Poisson point process Φ_p, i.e., $x_i \in \Phi_p$. Each base station x_i (the parent node) forms the center of a cluster, around which offspring points (near users) are uniformly distributed in a circle of radius R_c. The location of the cell-edge user can be set at the origin, since the considered PCP is a stationary and an isotropic point process. To reduce system complexity, we can set a finite region $\mathcal{D}$, for example, a disk with radius R centered at the origin. Only the BSs in $\mathcal{D}$ are invited to serve the cell-edge user. In the network NOMA transmission, each BS in $\mathcal{D}$ chooses a user from its offsprings as a near user, and sends the superimposed signal to serve the cell-edge user and the chosen near user simultaneously. The BSs outside $\mathcal{D}$ can be treated as interference sources. Analyzing the performance of the considered N-NOMA network with the above PCP model will be an important future direction.

APPENDIX A
PROOF FOR LEMMA1

In order to evaluate the outage probability P_0, we first fix the location of user 0, i.e., p_0. Given the fixed p_0, the distribution function of h_{i0} can be obtained. By using the property of the inequality in (9), we get the conditioned outage probability, and then finally we remove the condition on p_0.

A. Characterizing the Outage Probability With a Fixed p_0

Note that, as long as p_0 is fixed, L_{i0}, $1 \le i \le 3$, can be determined by p_0, and each $|h_{i0}|$, $1 \le i \le 3$, is Rayleigh distributed and independent to each other. The conditional pdf of each $|h_{i0}|$, given p_0, can be expressed as

$$f_{|h_{i0}|}(x\,|p_0\,) = 2L_{i0}xe^{-L_{i0}x^2}, x > 0. \tag{34}$$

The joint conditional pdf of $|h_{10}|$, $|h_{20}|$ and $|h_{30}|$ can be expressed as

$$f_{|h_{i0},|h_{20},|h_{30}|}(x,y,z\,|p_0\,) = 8L_{10}L_{20}L_{30}xyze^{-\left(L_{10}x^2+L_{20}y^2+L_{30}z^2\right)}. \tag{35}$$

Then the outage probability of user 0 can be formulated as

$$\begin{aligned} P_0 &= E_{p_0}\left\{ \iiint\limits_{(x,y,z)\in V} f_{|h_{i0},|h_{20},|h_{30}|}(x,y,z\,|p_0\,)\,dx\,dy\,dz \right\} \\ &= E_{p_0}\left\{ \iiint\limits_{(x,y,z)\in V} 8L_{10}L_{20}L_{30}xyz \right. \\ &\qquad \left. e^{-\left(L_{10}x^2+L_{20}y^2+L_{30}z^2\right)}\,dx\,dy\,dz \right\}, \end{aligned} \tag{36}$$

where

$$\begin{aligned} V = \Big\{ (x,y,z)\,\big|\big(\beta_0^2-\beta_1^2\eta_0\big)\left(x^2+y^2+z^2\right) \\ + 2\beta_0^2\left(xy+yz+xz\right) < \frac{\eta_0}{\rho}, x>0, y>0, z>0 \Big\} \end{aligned}$$

is the integral region. At high SNR, P_0 can be approximated as

$$\begin{aligned} P_0 &\approx E_{p_0}\left\{ \iiint\limits_{(x,y,z)\in V} 8L_{10}L_{20}L_{30}xyz\,dx\,dy\,dz \right\} \\ &= 8E_{p_0}\left\{L_{10}L_{20}L_{30}\right\} \iiint\limits_{(x,y,z)\in V} xyz\,dx\,dy\,dz. \end{aligned} \tag{37}$$

Note that, in this paper, as mentioned in Section III, we have assumed that $\beta_0^2 - \beta_1^2\eta_0 > 0$. The integral in (37) can be evaluated by treating first the integral with respect to x and y, z as constants. Then the integral can be written as

$$\begin{aligned} \iiint\limits_{(x,y,z)\in V} xyz\,dx\,dy\,dz &= \iint\limits_{(y,z)\in V_{yz}} \int_0^{X(y,z)} xyz\,dx\,dy\,dz \\ &= \underbrace{\frac{1}{2}\iint\limits_{(y,z)\in V_{yz}} X^2(y,z)yz\,dy\,dz}_{Q_1}, \end{aligned} \tag{38}$$

where $X(y,z)$ and V_{yz} are obtained from V by solving a quadratic inequality problem. The $X(y,z)$ can be expressed as

$$\begin{aligned} X(y,z) = \frac{1}{\beta_0^2-\beta_1^2\eta_0} \times \Bigg(\Big((2\beta_0^2\beta_1^2\eta_0 - \beta_1^4\eta_0^2)(y^2+z^2) \\ + 2\beta_0^2\beta_1^2\eta_0 yz + (\beta_0^2-\beta_1^2\eta_0)\eta_0/\rho \Big)^{1/2} - \beta_0^2(y+z) \Bigg), \end{aligned} \tag{39}$$

and V_{yz} as

$$\begin{aligned} V_{yz} = \Big\{ (y,z)\,\Big|\big(\beta_0^2-\beta_1^2\eta_0\big)\left(y^2+z^2\right) + 2\beta_0^2yz < \frac{\eta_0}{\rho}, \\ y>0, z>0 \Big\}. \end{aligned} \tag{40}$$

In order to simplify the notation of range of the integral, we use the following variable substitution

$$\begin{cases} y = -\dfrac{\sqrt{2}}{2}u + \frac{\sqrt{2}}{2}v \\ z = \dfrac{\sqrt{2}}{2}u + \frac{\sqrt{2}}{2}v. \end{cases} \tag{41}$$

Now the range of the integral, denoted by V_{uv}, can be easily derived from V_{yz} as

$$V_{uv} = \left\{ (u,v) \,\middle|\, \left(2\beta_0^2 - \beta_1^2\eta_0\right) v^2 - 2\beta_1^2\eta_0 u^2 < \tfrac{\eta_0}{\rho}, v > |u| \right\}. \tag{42}$$

Then the integral in (38) can be written as

$$Q_1 = \frac{1}{2} \iint\limits_{(u,v)\in V_{uv}} X^2(u,v)(v^2-u^2)\, du\, dv, \tag{43}$$

where $X(u,v)$ is derived from $X(y,z)$ and

$$\begin{aligned} X(u,v) = \frac{1}{\beta_0^2 - \beta_1^2\eta_0} \times \Bigg(& \Big((\beta_0^2\beta_1^2\eta_0 - \beta_1^4\eta_0^2)u^2 \\ & + (3\beta_0^2\beta_1^2\eta_0 - \beta_1^4\eta_0^2)v^2 + (\beta_0^2 - \beta_1^2\eta_0)\eta_0/\rho \Big)^{1/2} \\ & - \sqrt{2}\beta_0^2 v \Bigg). \end{aligned} \tag{44}$$

By further observation, the range of the integral can be decomposed into two parts:

- when $0 < v < \sqrt{\frac{\eta_0}{\rho\left(2\beta_0^2 - \beta_1^2\eta_0\right)}}$, the range of u is $-v < u < v$;
- when $\sqrt{\frac{\eta_0}{\rho\left(2\beta_0^2 - \beta_1^2\eta_0\right)}} < v < \sqrt{\frac{\eta_0}{\rho\left(2\beta_0^2 - 2\beta_1^2\eta_0\right)}}$, the range of u is $\sqrt{\frac{\left(2\beta_0^2 - \beta_1^2\eta_0\right)v^2 - \eta_0/\rho}{\beta_1^2\eta_0}} < |u| < v$.

Then Q_1 can be evaluated as

$$\begin{aligned} Q_1 = & \underbrace{\int_0^{\phi}\int_0^{v} X^2(u,v)(v^2-u^2)\, du\, dv}_{Q_{11}} \\ & + \underbrace{\int_{\phi}^{\phi_1}\int_{\varphi(v)}^{v} X^2(u,v)(v^2-u^2)\, du\, dv}_{Q_{12}}, \end{aligned} \tag{45}$$

where

$$\begin{cases} \phi_1 = \sqrt{\frac{\eta_0}{\rho\left(2\beta_0^2 - 2\beta_1^2\eta_0\right)}} \\ \varphi(v) = \sqrt{\frac{\left(2\beta_0^2 - \beta_1^2\eta_0\right)v^2 - \eta_0/\rho}{\beta_1^2\eta_0}}. \end{cases}$$

An interesting observation is that the second part integral is much smaller than the first part, i.e., $Q_{11} >> Q_{12}$. Thus Q_1 can be approximated as

$$Q_1 \approx \textstyle\int_0^{\phi}\int_0^{v} X^2(u,v)(v^2-u^2)\, du\, dv. \tag{46}$$

After some manipulations, we get

$$Q_1 \approx \frac{1}{(\beta_0^2 - \beta_1^2\eta_0)^2}\left(G(\phi) - F(\phi) + F(0)\right). \tag{47}$$

Then, the outage probability at user 0 can be expressed as

$$P_0 = 4Q_1 E_{p_0}\left\{L_{10}L_{20}L_{30}\right\}. \tag{48}$$

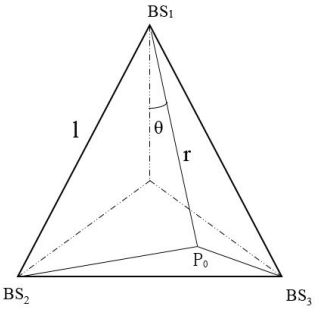

Fig. 12. Distances between BSs and user 0.

B. Removing the Condition on p_0

The next step of the proof is to remove the condition on the location of user 0. To accomplish this, recall that user 0 is uniformly distributed in the intersecting area of the three discs, i.e., A. Therefore, the above expectation with respect to p_0 can be written as

$$\begin{aligned} E_{p_0}\left\{L_{10}L_{20}L_{30}\right\} &= \int_{p_0\in A} L_{10}L_{20}L_{30}\frac{1}{S_A}\, dp_0 \\ &= \frac{1}{S_A}\int_{p_0\in A} L_{10}L_{20}L_{30}\, dp_0, \end{aligned} \tag{49}$$

where S_A is the area of A. Furthermore, recall that A is composed of A_1, A_2 and A_3 as illustrated in Fig. 1. Due to the symmetry of A_1, A_2 and A_3, the expectation can be further formulated as

$$\begin{aligned} E_{p_0}\left\{L_{10}L_{20}L_{30}\right\} &= \frac{1}{3}\left(\frac{1}{S_{A_1}}\int_{p_0\in A_1} L_{10}L_{20}L_{30}\, dp_0 \right. \\ &\quad + \frac{1}{S_{A_2}}\int_{p_0\in A_2} L_{10}L_{20}L_{30}\, dp_0 \\ &\quad \left. + \frac{1}{S_{A_3}}\int_{p_0\in A_3} L_{10}L_{20}L_{30}\, dp_0 \right) \\ &= \frac{1}{S_{A_1}}\int_{p_0\in A_1} L_{10}L_{20}L_{30}\, dp_0, \end{aligned} \tag{50}$$

where S_{A_1} is the area of A_1, given by

$$\begin{aligned} S_{A_1} &= \frac{1}{3}S_A \\ &= R_0^2\left(\frac{\pi}{3} - \arcsin\left(\frac{l}{2R_0}\right)\right) \\ &\quad - \frac{\sqrt{3}}{3}lR_0\sin\left(\frac{\pi}{3} - \arcsin\left(\frac{l}{2R_0}\right)\right). \end{aligned} \tag{51}$$

After transforming to polar coordinates, as shown in Fig. 12, L_{10}, L_{20} and L_{30} can be expressed as

$$\begin{cases} L_{10} = r^{\alpha} \\ L_{20} = (l^2 + r^2 - 2lr\cos(\pi/6 + \theta))^{\frac{\alpha}{2}} \\ L_{30} = (l^2 + r^2 - 2lr\cos(\pi/6 - \theta))^{\frac{\alpha}{2}}, \end{cases} \tag{52}$$

which are obtained by using the law of cosines. Then, the expectation can be written as

$$E_{p_0}\left\{L_{10}L_{20}L_{30}\right\} = \tfrac{1}{S_{A_1}}\textstyle\int_{\frac{\sqrt{3}}{3}l}^{R_0}\int_{-\Theta}^{+\Theta} L_{10}L_{20}L_{30}r\, d\theta\, dr, \tag{53}$$

where $\Theta = \frac{\pi}{3} - \arcsin\left(\frac{l}{2r}\right)$.

After some algebraic manipulations, the expectation expression in (11) for $\alpha = 2$ can be obtained. For the case when $\alpha > 2$, we only focus on the scenario when $\frac{R_0}{l} \to \frac{\sqrt{3}}{3}$, which yields $\theta \to 0$. By using Taylor series, the product of L_{10}, L_{20} and L_{30} can be expressed as

$$\begin{aligned} &L_{10}L_{20}L_{30} \\ &= \frac{1}{2}\alpha\left(\sqrt{3}l^3r^3 - 4l^2r^4 + \sqrt{3}lr^5\right) \\ &\quad + \left(l^4r^2 - 2\sqrt{3}l^3r^3 + 5l^2r^4 - 2\sqrt{3}lr^5 + r^6\right)^{\alpha/2} + O(\theta^2) \\ &\triangleq \tilde{Q}_1 + O(\theta^2), \end{aligned} \tag{54}$$

thus, (53) can be further calculated as

$$E_{p_0}\left\{L_{10}L_{20}L_{30}\right\} \approx \frac{1}{S_{A_1}} \int_{\frac{\sqrt{3}}{3}l}^{R_0} 2\Theta\tilde{Q}_1 r\, dr, \tag{55}$$

Replacing r with x in (55), where $r = (\frac{\sqrt{3}}{3} + x)l$. Note that when $\frac{R_0}{l} \to \frac{\sqrt{3}}{3}$, $x \to 0$. Thus we get the following approximation:

$$2\Theta\tilde{Q}_1 r \approx 2 \times 3^{\frac{1}{2}-\frac{3\alpha}{2}} l^{3\alpha+1} x \tag{56}$$

which is obtained by using Taylor series. Then $E_{p_0}\left\{L_{10}L_{20}L_{30}\right\}$ can be calculated as

$$\begin{aligned} E_{p_0}\left\{L_{10}L_{20}L_{30}\right\} &\approx \frac{1}{S_{A_1}} \int_0^{\frac{R_0}{l}-\frac{\sqrt{3}}{3}} 2 \times 3^{\frac{1}{2}-\frac{3\alpha}{2}} l^{3\alpha+2} x\, dx, \\ &= \frac{\sqrt{3}(R_0 - \frac{\sqrt{3}}{3}l)^2 \times 3^{-\frac{3\alpha}{2}} l^{3\alpha}}{S_{A_1}} \\ &\overset{(a)}{\approx} 3^{-\frac{3\alpha}{2}} l^{3\alpha} \end{aligned} \tag{57}$$

where (a) follows from the fact that S_{A_1} can be approximated as $S_{A_1} \approx \sqrt{3}\left(R_0 - \frac{\sqrt{3}}{3}l\right)^2$, when $\frac{R_0}{l} \to \sqrt{3}/3$. Therefore Lemma 1 is proved.

Appendix B
Proof for Lemma 2

The received signal can be expressed as

$$\tilde{y}_0 = \sqrt{\sum_{i=1}^{3} |h_{i0}|^2 \sqrt{3P_s} s_0 + n_0} \tag{58}$$

and the received SNR as

$$\text{SNR} = \frac{3P_s \sum_{i=1}^{3} |h_{i0}|^2}{\sigma^2} = 3\rho \sum_{i=1}^{3} |h_{i0}|^2. \tag{59}$$

Then, the outage probability is given by

$$\begin{aligned} \tilde{P}_0 &= P\left(\log\left(1 + 3\rho\sum_{i=1}^{3}|h_{i0}|^2\right) < r_0\right) \\ &= P\left(\sum_{i=1}^{3}|h_{i0}|^2 < \frac{\eta_0}{3\rho}\right). \end{aligned} \tag{60}$$

The key step to calculate $\tilde{P}_0$ is to obtain the pdf of $\sum_{i=1}^{3}|h_{i0}|^2$. Note that, as long as the location of user 0 (p_0) is fixed, L_{i0}, $1 \le i \le 3$, can be determined by p_0, and the pdf of $|h_{i0}|^2$ given p_0 follows exponential distribution, i.e., $f_{|h_{i0}^2|}(x|p_0) = L_{i0}e^{-L_{i0}x}$. Define $\psi = \sum_{i=1}^{3}|h_{i0}|^2$. Note that if $L_{10} \neq L_{20} \neq L_{30}$, then the pdf of ψ is given by

$$f_\psi(x|p_0) = \sum_{i=1}^{3} L_{i0}e^{-L_{i0}x} \prod_{\substack{j=1 \\ j\neq i}}^{3} \frac{L_{j0}}{L_{j0} - L_{i0}}. \tag{61}$$

Thus the outage probability can be calculated as follows:

$$\begin{aligned} \tilde{P}_0 &= E_{p_0}\left\{\int_0^{\frac{\eta_0}{3\rho}} f_\psi(x|p_0)\, dx\right\} \\ &= E_{p_0}\underbrace{\left\{\sum_{i=1}^{3}\left(1 - e^{-L_{i0}\frac{\eta_0}{3\rho}}\right)\prod_{\substack{j=1 \\ j\neq i}}^{3}\frac{L_{j0}}{L_{j0}-L_{i0}}\right\}}_{Q_3}. \end{aligned} \tag{62}$$

By changing to polar coordinates, the above expectation with respect to p_0 can be evaluated as

$$\tilde{P}_0 = \frac{1}{S_{A_1}} \int_{\frac{\sqrt{3}}{3}l}^{R_0} \int_{-\Theta}^{\Theta} Q_3\, r dr d\theta, \tag{63}$$

where Q_3 is a function of r and θ, and $\Theta = \frac{\pi}{3} - \arcsin\left(\frac{l}{2r}\right)$. Note that, we only focus of the scenario of $k \to \sqrt{3}/3$, which yields $\theta \to 0$. By using the Taylor series, Q_3 can be approximated as

$$\begin{aligned} Q_3 \approx{}& \frac{r^\alpha e^{-tT}\left(r^\alpha\left(e^{tT}-1\right) - T\left(tr^\alpha + 2e^{tT} - 2\right) + tT^2\right)}{\left(T - r^\alpha\right)^2} \\ &+ \frac{T^2\left(1 - e^{t(-r^\alpha)}\right)}{\left(T - r^\alpha\right)^2} \triangleq \tilde{Q}_3, \end{aligned} \tag{64}$$

where $T = \left(l^2 - \sqrt{3}lr + r^2\right)^{\alpha/2}$. Note that $\tilde{Q}_3$ is a function of only r. Then (63) can be further written as

$$\tilde{P}_0 \approx \frac{1}{S_{A_1}} \int_{\frac{\sqrt{3}}{3}l}^{R_0} \int_{-\Theta}^{\Theta} \tilde{Q}_3\, r dr d\theta \approx \frac{1}{S_{A_1}} \int_{\frac{\sqrt{3}}{3}l}^{R_0} 2\Theta\tilde{Q}_3\, r dr. \tag{65}$$

Replacing r with x in (65), where $r = \frac{\sqrt{3}}{3}l(1+x)$. Note that when $k \to \sqrt{3}/3$, $x \to 0$. Thus we get the following approximation:

$$\begin{aligned} 2\Theta\tilde{Q}_3 r \approx{}& \frac{\sqrt{3}lxe^{-\frac{3^{-\frac{\alpha}{2}-1}\eta_0 l^\alpha}{\rho}}}{3^{\alpha+2}\rho^2} \\ &\times\Bigg(-\eta_0^2 l^{2\alpha} + 2 \times 3^{\alpha+2}\rho^2\left(e^{\frac{3^{-\frac{\alpha}{2}-1}\eta_0 l^\alpha}{\rho}} - 1\right) \\ &-2 \times 3^{\frac{\alpha}{2}+1}\eta_0\rho l^\alpha\Bigg), \end{aligned} \tag{66}$$

which is obtained by using the Taylor series and omitting terms of higher order. Then $\tilde{P}_0$ can be expressed after some algebraic manipulations as

$$\begin{aligned} \tilde{P}_0 \approx{}& \frac{e^{-\frac{3^{-\frac{\alpha}{2}-1}\eta_0 l^\alpha}{\rho}}\sqrt{3}\left(R_0 - \frac{\sqrt{3}}{3}l\right)^2}{2 \times 3^{\alpha+2}\rho^2 S_{A_1}} \times \Bigg(-2 \times 3^{\frac{\alpha}{2}+1}\eta_0\rho l^\alpha \\ &- \eta_0^2 l^{2\alpha} + 2 \times 3^{\alpha+2}\rho^2\left(e^{\frac{3^{-\frac{\alpha}{2}-1}\eta_0 l^\alpha}{\rho}} - 1\right)\Bigg) \\ \overset{(a)}{\approx}{}& \frac{e^{-\frac{3^{-\frac{\alpha}{2}-1}\eta_0 l^\alpha}{\rho}}}{2 \times 3^{\alpha+2}\rho^2} \times \Bigg(-2 \times 3^{\frac{\alpha}{2}+1}\eta_0\rho l^\alpha - \eta_0^2 l^{2\alpha} + 2 \\ &\times 3^{\alpha+2}\rho^2\left(e^{\frac{3^{-\frac{\alpha}{2}-1}\eta_0 l^\alpha}{\rho}} - 1\right)\Bigg) \end{aligned} \tag{67}$$

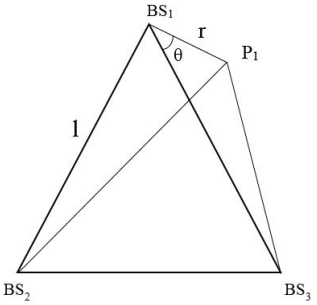

Fig. 13. Distances between BSs and user 1.

where (a) follows from the fact that S_{A_1} can be approximated as $S_{A_1} \approx \sqrt{3}\left(R_0 - \frac{\sqrt{3}}{3}l\right)^2$, when $k \to \sqrt{3}/3$. Therefore, Lemma 2 is proved.

APPENDIX C
PROOF FOR LEMMA 3

Without loss of generality, the following derivation process focus on calculating the outage probability achieved by user 1.

Recall that $\left|\tilde{h}_{jj}\right|^2$ is exponentially distributed, i.e., the pdf of $\left|\tilde{h}_{jj}\right|^2$ is $f_{\left|\tilde{h}_{jj}\right|^2}(x) = L_{ij}e^{-L_{ij}x}$. Then, the outage probability at user 1 can be calculated as

$$P_1 = E_{p_1,|\tilde{h}_{21}|^2,|\tilde{h}_{31}|^2}\left\{1 - e^{-L_{11}M_1\left[\left(|\tilde{h}_{21}|^2+|\tilde{h}_{31}|^2\right)\beta_1^2+1/\rho\right]}\right\}. \tag{68}$$

By using (68), the outage probability at user 1 can be expressed as

$$P_1 = 1 - E_{p_1}\left\{e^{-\frac{L_{11}M_1}{\rho}} \times \underbrace{\frac{L_{21}}{L_{11}M_1\beta_1^2 + L_{21}} \times \frac{L_{31}}{L_{11}M_1\beta_1^2 + L_{31}}}_{Q_2}\right\}. \tag{69}$$

Then, the expectation part can be evaluated as

$$E_{p_1}\left\{Q_2 e^{-\frac{L_{11}M_1}{\rho}}\right\} = \frac{1}{\pi R_1^2}\int_{p_1\in D_1} Q_2 e^{-\frac{L_{11}M_1}{\rho}}\, dp_1 \overset{(a)}{=} \frac{1}{\pi R_1^2}\int_0^{2\pi}\int_0^{R_1} Q_2 e^{-\frac{L_{11}M_1}{\rho}} r\; drd\theta, \tag{70}$$

where (a) follows a step changing to polar coordinates, as shown in Fig. 13. Note that L_{11}, L_{21} and L_{31} can be expressed as

$$\begin{cases} L_{11} = r^\alpha \\ L_{21} = \left(r^2 + l^2 - 2lr\cos\left(\pi/3+\theta\right)\right)^{\frac{\alpha}{2}} \\ L_{31} = \left(r^2 + l^2 - 2lr\cos\left(\theta\right)\right)^{\frac{\alpha}{2}} \end{cases}. \tag{71}$$

Then, Q_2 can be formulated as

$$\begin{aligned} Q_2 &= \left(1 - \frac{M_1\beta_1^2 L_{11}}{M_1\beta_1^2 L_{11} + L_{21}}\right) \times \left(1 - \frac{M_1\beta_1^2 L_{11}}{M_1\beta_1^2 L_{11} + L_{31}}\right) \\ &= \left(1 - \frac{M_1\beta_1^2 r^\alpha}{M_1\beta_1^2 r^\alpha + \left(r^2 + l^2 - 2lr\cos\left(\pi/3+\theta\right)\right)^{\frac{\alpha}{2}}}\right) \\ &\quad \times \left(1 - \frac{M_1\beta_1^2 r^\alpha}{M_1\beta_1^2 r^\alpha + \left(r^2 + l^2 - 2lr\cos\left(\theta\right)\right)^{\frac{\alpha}{2}}}\right) \end{aligned} \tag{72}$$

When $R_2 << l$, Q_2 can be approximated as

$$Q_2 \approx 1 - 2\beta_1^2 M_1 \frac{r^\alpha}{l^\alpha}, \tag{73}$$

which is obtained by the using Taylor series. Then the above expectation can be written as

$$\begin{aligned} &E_{p_1}\left\{Q_2 e^{-\frac{L_{11}M_1}{\rho}}\right\} \\ &\approx \frac{1}{\pi R_1^2}\int_0^{2\pi}\int_0^{R_1}\left(1 - 2\beta_1^2 M_1\frac{r^\alpha}{l^\alpha}\right)e^{-\frac{r^\alpha M_1}{\rho}} r\; drd\theta \\ &= \frac{2\rho^{\frac{2}{\alpha}}M_1\gamma(\frac{2}{\alpha}, \frac{M_1R_1^\alpha}{\rho}) - \frac{4\beta_1^2M_1\rho^{\frac{2}{\alpha}+1}}{l^\alpha}\gamma(\frac{2}{\alpha}+1, \frac{M_1R_1^\alpha}{\rho})}{\alpha M_1^{\frac{2}{\alpha}+1}R_1^2}. \end{aligned} \tag{74}$$

So, the outage probability at user 1 can be expressed as

$$P_1 \approx 1 - \frac{2\rho^{\frac{2}{\alpha}}M_1\gamma(\frac{2}{\alpha}, \frac{M_1R_1^\alpha}{\rho}) - \frac{4\beta_1^2M_1\rho^{\frac{2}{\alpha}+1}}{l^\alpha}\gamma(\frac{2}{\alpha}+1, \frac{M_1R_1^\alpha}{\rho})}{\alpha M_1^{\frac{2}{\alpha}+1}R_1^2}, \tag{75}$$

By replacing the subscript of 1 with j, Lemma 3 is proved.

APPENDIX D
PROOF FOR LEMMA 4

As in Appendix C, this appendix focuses on calculating the outage probability achieved by user 1. Following the similar steps as in Appendix C, P_1^{Inter} can be expressed as

$$P_1^{\text{Inter}} = 1 - E_{p_1}\left\{E_{I_1}\left\{e^{-L_{11}M_1I_1}\right\}e^{-\frac{L_{11}M_1}{\rho}} \times \underbrace{\frac{L_{21}}{L_{11}M_1\beta_1^2 + L_{21}} \times \frac{L_{31}}{L_{11}M_1\beta_1^2 + L_{31}}}_{Q_2}\right\}. \tag{76}$$

Note that, $E_{I_1}\left\{e^{-L_{11}M_1I_1}\right\}$ can be evaluated as

$$\begin{aligned} &E_{I_1}\left\{e^{-L_{11}M_1I_1}\right\} \\ &= E_{\Phi_I, g_{I_k,1}}\left\{\prod_{p_{I_k}\in\Phi_I}\exp\left(-L_{11}M_1\rho_I\frac{|g_{I_k,j}|^2}{L(||p_{I_k}-p_1||)}\right)\right\} \\ &= E_{\Phi_I}\left\{\prod_{p_{I_k}\in\Phi_I}\frac{1}{\frac{L_{11}M_1\rho_I}{L(||p_{I_k}-p_1||)}+1}\right\}. \end{aligned} \tag{77}$$

By applying Campell theorem and the PFGL, $E_{I_1}\left\{e^{-L_{11}M_1I_1}\right\}$ can be calculated as

$$E_{I_1}\left\{e^{-L_{11}M_1I_1}\right\} = \exp\left(-\lambda_I\int_{R^2}\left(1 - \frac{1}{\frac{L_{11}M_1\rho_I}{L(||p-p_1||)}+1}\right)dp\right). \tag{78}$$

By doing the substitution $p' = p - p_1$, we have

$$E_{I_1}\left\{e^{-L_{11}M_1I_1}\right\} = \exp\left(-\lambda_I\int_{R^2}\left(1 - \frac{1}{\frac{L_{11}M_1\rho_I}{L(||p'||)}+1}\right)dp'\right)$$

$$= \exp\left(-\lambda_I \int_0^{2\pi}\int_0^{\infty}\left(1-\frac{1}{\frac{L_{11}M_1\rho_I}{r^\alpha}+1}\right) r\, dr d\theta\right)$$
$$= \exp\left(-2\pi\lambda_I \int_0^{\infty}\frac{L_{11}M_1\rho_I r}{L_{11}M_1\rho_I + r^\alpha}\, dr\right)$$
$$= \exp\left(-2\pi\lambda_I \frac{(L_{11}M_1\rho_I)^{\frac{2}{\alpha}}}{\alpha} B\left(\frac{2}{\alpha}, 1-\frac{2}{\alpha}\right)\right), \quad (79)$$

where the last step is obtained by applying Beta function. Again changing to polar coordinates and using the the approximation as in (73), P_1^{Inter} can be approximated as

$$P_1^{\text{Inter}} \approx 1 - \frac{1}{\pi R_1^2}\int_0^{2\pi}\int_0^{R_1}\left(1-2\beta_1^2 M_1 \frac{r^\alpha}{l^\alpha}\right) \times \exp\left(-\frac{M_1}{\rho}r^\alpha - 2\pi\lambda_I \frac{(M_1\rho_I)^{\frac{2}{\alpha}}}{\alpha} B\left(\frac{2}{\alpha}, 1-\frac{2}{\alpha}\right) r^2\right) r\, dr d\theta. \quad (80)$$

By Applying Gauss-Chebyshev quadrature and substituting the subscript 1 with j, Lemma 4 follows.

REFERENCES

[1] Y. Saito, Y. Kishiyama, A. Benjebbour, T. Nakamura, A. Li, and K. Higuchi, "Non-orthogonal multiple access (NOMA) for cellular future radio access," in *Proc. IEEE Veh. Technol. Conf.*, Dresden, Germany, Jun. 2013, pp. 1–5.

[2] Z. Ding *et al.*, "Application of non-orthogonal multiple access in LTE and 5G networks," *IEEE Commun. Mag.*, vol. 55, no. 2, pp. 185–191, Feb. 2017.

[3] B. Kim *et al.*, "Non-orthogonal multiple access in a downlink multiuser beamforming system," in *Proc. IEEE Military Commun. Conf. (MILCOM)*, Nov. 2013, pp. 1278–1283.

[4] T. M. Cover and J. A. Thomas, *Elements of Information Theory*, 2nd ed. Hoboken, NJ, USA: Wiley, 2006.

[5] J. Choi, "Minimum power multicast beamforming with superposition coding for multiresolution broadcast and application to NOMA systems," *IEEE Trans. Commun.*, vol. 63, no. 3, pp. 791–800, Mar. 2015.

[6] K. Higuchi and A. Benjebbour, "Non-orthogonal multiple access (NOMA) with successive interference cancellation for future radio access," *IEICE Trans. Commun.*, vol. 98, no. 3, pp. 403–414, 2015.

[7] Z. Ding, Z. Yang, P. Fan, and H. V. Poor, "On the performance of non-orthogonal multiple access in 5G systems with randomly deployed users," *IEEE Signal Process. Lett.*, vol. 21, no. 12, pp. 1501–1505, Dec. 2014.

[8] S. Timotheou and I. Krikidis, "Fairness for non-orthogonal multiple access in 5G systems," *IEEE Signal Process. Lett.*, vol. 22, no. 10, pp. 1647–1651, Oct. 2015.

[9] Z. Ding *et al.*, "Impact of user pairing on 5G nonorthogonal multiple-access downlink transmissions," *IEEE Trans. Veh. Technol.*, vol. 65, no. 8, pp. 6010–6023, Aug. 2016.

[10] M. Al-Imari, P. Xiao, M. A. Imran, and R. Tafazolli, "Uplink non-orthogonal multiple access for 5G wireless networks," in *Proc. 11th Int. Symp. Wireless Commun. Sys.*, Aug. 2014, pp. 781–785.

[11] Z. Ding, F. Adachi, and H. V. Poor, "The application of MIMO to non-orthogonal multiple access," *IEEE Trans. Wireless Commun.*, vol. 15, no. 1, pp. 537–552, Jan. 2016.

[12] Q. Sun, S. Han, C. L. I, and Z. Pan, "On the ergodic capacity of MIMO NOMA systems," *IEEE Wireless Commun. Lett.*, vol. 4, no. 4, pp. 405–408, Aug. 2015.

[13] Z. Ding, R. Schober, and H. V. Poor, "A general MIMO framework for NOMA downlink and uplink transmission based on signal alignment," *IEEE Trans. Wireless Commun.*, vol. 15, no. 6, pp. 4438–4454, Jun. 2016.

[14] Z. Ding, L. Dai, R. Schober, and H. V. Poor, "NOMA meets finite resolution analog beamforming in massive MIMO and millimeter-wave networks," *IEEE Commun. Lett.*, vol. 21, no. 8, pp. 1879–1882, Aug. 2017.

[15] H. Marshoud, V. M. Kapinas, G. K. Karagiannidis, and S. Muhaidat, "Non-orthogonal multiple access for visible light communications," *IEEE Photon. Technol. Lett.*, vol. 28, no. 1, pp. 51–54, Jan. 1, 2016.

[16] H. Huang, M. Trivellato, A. Hottinen, M. Shafi, P. J. Smith, and R. Valenzuela, "Increasing downlink cellular throughput with limited network MIMO coordination," *IEEE Trans. Wireless Commun.*, vol. 8, no. 6, pp. 2983–2989, Jun. 2009.

[17] S. Venkatesan, A. Lozano, and R. Valenzuela, "Network MIMO: Overcoming intercell interference in indoor wireless systems," in *Proc. Conf. Rec. 41st Asilomar Conf. Signals, Syst. Comput. (ACSSC)*, Nov. 2007, pp. 83–87.

[18] V. Jungnickel *et al.*, "Coordinated multipoint trials in the downlink," in *Proc. IEEE Globecom. Workshops*, Honolulu, HI, USA, Dec. 2009, pp. 1–7.

[19] M. Sawahashi, Y. Kishiyama, A. Morimoto, D. Nishikawa, and M. Tanno, "Coordinated multipoint transmission/reception techniques for LTE-advanced [Coordinated and Distributed MIMO]," *IEEE Wireless Commun.*, vol. 17, no. 3, pp. 26–34, Jun. 2010.

[20] R. Irmer *et al.*, "Coordinated multipoint: Concepts, performance, and field trial results," *IEEE Commun. Mag.*, vol. 49, no. 2, pp. 102–111, Feb. 2011.

[21] L. Venturino, N. Prasad, and X. Wang, "Coordinated linear beamforming in downlink multi-cell wireless networks," *IEEE Trans. Wireless Commun.*, vol. 9, no. 4, pp. 1451–1461, Apr. 2010.

[22] H. Dahrouj and W. Yu, "Coordinated beamforming for the multicell multi-antenna wireless system," *IEEE Trans. Wireless Commun.*, vol. 9, no. 5, pp. 1748–1759, May 2010.

[23] J. Choi, "Non-orthogonal multiple access in downlink coordinated two-point systems," *IEEE Commun. Lett.*, vol. 18, no. 2, pp. 313–316, Feb. 2014.

[24] Y. Tian *et al.*, "On the performance of opportunistic NOMA in downlink CoMP networks," *IEEE Commun. Lett.*, vol. 20, no. 5, pp. 998–1001, May 2016.

[25] S. M. Alamouti, "A simple transmit diversity technique for wireless communications," *IEEE J. Sel. Areas Commun.*, vol. 16, no. 8, pp. 1451–1458, Oct. 1988.

[26] *Study on Downlink Multiuser Superposition Transmission for LTE*, document R1-153638, 3rd Generation Partnership Project, Mar. 2015.

[27] H. Tabassum, E. Hossain, and J. Hossain, "Modeling and analysis of uplink non-orthogonal multiple access in large-scale cellular networks using poisson cluster processes," *IEEE Trans. Commun.*, vol. 65, no. 8, pp. 3555–3570, Aug. 2017.

Yanshi Sun received the B.S. degree from the University of Science and Technology of China in 2016, where he is currently pursuing the master's degree with the Department of Electronic Engineering and Information Science. His current research interests include stochastic geometry and non-orthogonal multiple access (NOMA) systems.

Zhiguo Ding (S'03–M'05–SM'15) received the B.Eng. degree in electrical engineering from the Beijing University of Posts and Telecommunications in 2000, and the Ph.D. degree in electrical engineering from Imperial College London in 2005. From 2005 to 2018, he was with Queens University Belfast, Imperial College, Newcastle University, and Lancaster University. Since 2018, he has been with the University of Manchester as a Professor in communications. From 2012 to 2016, he was with Princeton University as an Academic Visitor. His research interests include 5G networks, game theory, cooperative and energy harvesting networks, and statistical signal processing. He is serving as an Editor for the IEEE TRANSACTIONS ON COMMUNICATIONS, the IEEE TRANSACTIONS ON VEHICULAR NETWORKS, the IEEE WIRELESS COMMUNICATION LETTERS, the IEEE COMMUNICATION LETTERS, and the *Journal of Wireless Communications and Mobile Computing*. He received the Best Paper Award from the IET Communication Conference on Wireless, Mobile and Computing, in 2009, the IEEE COMMUNICATION LETTER Exemplary Reviewer 2012, and the EU Marie Curie Fellowship from 2012 to 2014.

Xuchu Dai received the B.Eng. degree in electrical engineering from the Airforce Engineering University, Xi'an, China, in 1984, and the M.Eng. and Ph.D. degrees in communication and information system from the University of Science and Technology of China, Hefei, China, in 1991 and 1998, respectively. He is currently a Professor with the Department of Electronic Engineering and Information Science, University of Science and Technology of China. From 2000 to 2002, he was with The Hong Kong University of Science and Technology as a Post-Doctoral Researcher. His current research interests include wireless communication systems, blind adaptive signal processing, and signal detection.

George K. Karagiannidis (M'96–SM'03–F'14) was born in Pithagorion, Greece. He received the University Diploma and Ph.D. degrees in electrical and computer engineering from the University of Patras in 1987 and 1999, respectively. From 2000 to 2004, he was a Senior Researcher at the Institute for Space Applications and Remote Sensing, National Observatory of Athens, Greece. In 2004, he joined the Faculty of Aristotle University of Thessaloniki, Greece, where he is currently a Professor with the Electrical and Computer Engineering Department and the Director of the Digital Telecommunications Systems and Networks Laboratory. He is also an Honorary Professor at South West Jiaotong University, Chengdu, China.

His research interests include the broad area of digital communications systems and signal processing, with emphasis on wireless communications, optical wireless communications, wireless power transfer and applications, molecular and nanoscale communications, stochastic processes in biology and wireless security.

He is an author or co-author of over 450 technical papers published in scientific journals and presented at international conferences. He is also an author of the Greek edition of a book *Telecommunications Systems* and a co-author of the book *Advanced Optical Wireless Communications Systems* (Cambridge, 2012).

Dr. Karagiannidis has been the general chair, the technical program chair, and a member of technical program committees in several IEEE and non-IEEE conferences. He was an Editor of the IEEE TRANSACTIONS ON COMMUNICATIONS, a Senior Editor of the IEEE COMMUNICATIONS LETTERS, an Editor of the *EURASIP Journal of Wireless Communications and Networks*, and a several times Guest Editor of the IEEE *Selected Areas in Communications*. From 2012 to 2015, he was the Editor-in Chief of the IEEE COMMUNICATIONS LETTERS.

Dr. Karagiannidis is one of the highly cited authors across all areas of electrical engineering, recognized as a 2015, 2016, and 2017 Web-of-Science Highly Cited Researcher.